Microchimica Acta (2018) 185: 213
https://doi.org/10.1007/s00604-018-2750-5

REVIEW ARTICLE

A review on chemiresistive room temperature gas sensors based on metal oxide nanostructures, graphene and 2D transition metal dichalcogenides

Nirav Joshi[1,2] · Takeshi Hayasaka[1] · Yumeng Liu[1] · Huiliang Liu[1,3] · Osvaldo N. Oliveira Jr[2] · Liwei Lin[1,3]

Received: 25 December 2017 / Accepted: 26 February 2018 / Published online: 10 March 2018

Abstract

Room-temperature (RT) gas sensing is desirable for battery-powered or self-powered instrumentation that can monitor emissions associated with pollution and industrial processes. This review (with 171 references) discusses recent advances in three types of porous nanostructures that have shown remarkable potential for RT gas sensing. The first group comprises hierarchical oxide nanostructures (mainly oxides of Sn, Ni, Zn, W, In, La, Fe, Co). The second group comprises graphene and its derivatives (graphene, graphene oxides, reduced graphene oxides, and their composites with metal oxides and noble metals). The third group comprises 2D transition metal dichalcogenides (mainly sulfides of Mo, W, Sn, Ni, also in combination with metal oxides). They all have been found to enable RT sensing of gases such as NOx, NH_3, H_2, SO_2, CO, and of vapors such as of acetone, formaldehyde or methanol. Attractive features also include high selectivity and sensitivity, long-term stability and affordable costs. Strengths and limitations of these materials are highlighted, and prospects with respect to the development of new materials to overcome existing limitations are discussed.

Keywords Nanosensors, 2D Materials · Thin Films · Selectivity · Sensitivity · Surface reaction · Gas sensors · Semiconductors · Chemiresistive gas sensors

Introduction

Gas sensing technologies play a crucial role in applications that affect our daily life, such as in monitoring the environment and the air quality, in addition to detecting toxic gases [1–8]. Gas sensors of various types have been employed but the most popular ones are resistivity-based sensors owing to their low-cost fabrication, smooth operation and possible miniaturization [9–15]. The first commercial gas sensor produced in 1923 was based on a hot platinum wire, while the first oxide-based gas sensor was patented by Taguchi in 1962. Since the pioneering work by Seyama with gas sensors made by ZnO thin films and a basic electrical circuit operating at 485 °C [16], efforts have been made to improve sensitivity, stability and selectivity. With nanotechnology, it has been possible to make significant progresses with oxide nanostructures, conducting polymers, carbon nanostructures and 2D materials. This progress is reflected in the increasing number of scientific articles published, as shown in Fig. 1, particularly in the past few years.

In spite of the many advances of late, the search for reliable, robust gas sensors is an ongoing endeavor, and much more is expected for the next decade [17–23]. Improvements are continuously sought in the figures of merit that include sensor response, selectivity, stability and response/recovery speed, for which research is performed in novel materials, especially derived from nanotechnology [24–29, 18]. Efforts are particularly directed toward decreasing the operation temperature of such sensors [5, 6, 30, 31]. Traditional gas sensors made of metal oxides, for instance, normally operate at 100–400 °C, leading to high power consumption and reduced sensor stability and lifetime owing to an induced growth of metal oxide grains [32–35]. Gas sensors produced with conducting polymers can operate at room temperature, but they are affected by humidity being amenable to degradation with a sluggish response and recovery time, and poor stability [36–38].

✉ Nirav Joshi
nirav.joshi@berkeley.edu

[1] Department of Mechanical Engineering, University of California, Berkeley, CA 94720, USA

[2] São Carlos Institute of Physics, University of São Paulo, 369, São Carlos, São Paulo, CP 13560-970, Brazil

[3] Tsinghua-Berkeley Shenzhen Institute, Shenzhen 518055, China

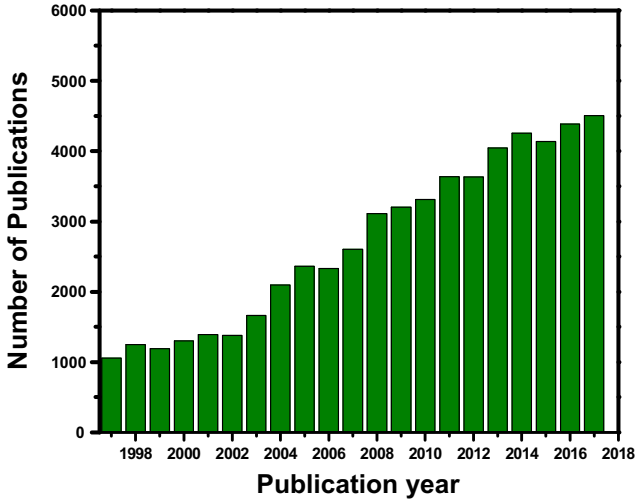

Fig. 1 The number of publications in the area of gas sensors from 1997 to 2017 (internet search of the Scopus on Jan. 29, 2018). Keywords for search: gas sensor

Strategies to improve sensitivity and selectivity have been developed, including surface functionalization with noble metals, the use of oxide heterostructures and thermal assistance with UV-illumination or an external heater [39–44, 30]. However, high operating temperatures and/or lack of stability of sensor devices are still major limitations. A primary challenge for this research field is, therefore, to design and develop robust, reliable gas sensors that are highly sensitive and selective to target gases, which can be operated at or close to room temperature under the influences of humidity. Various review articles and book chapters have addressed many issues involved in gas sensors [45–48], and therefore the aim is not to present a comprehensive survey of the achievements and prospects in the field. Rather, the focus here is on oxide nanostructures [12, 49–53], graphene and layered inorganic 2D materials [54–56, 46] for room temperature gas sensing, in view of their promising recent results. Our main motivation is to provide a short summary of recent developments with promising materials, and present an outlook for the next few years. The article has been divided into three sections, each of which corresponds to a class of these materials.

Materials for gas sensors operating at room temperature

Oxide nanostructures

Oxide nanostructures have been used in solar cells, sensors and biosensors, energy storage, drug delivery and dielectric/piezoelectric systems [57–63]. Metal oxides may adopt various shapes such as nanowires, nanotubes and nanobelts for gas sensing at room temperature [64–69], as illustrated in the parameters summarized in Table 1. The sensor response or sensitivity of materials is evaluated as $\left|\frac{\Delta R}{R_a}\right| \times 100$, where $\Delta R = R_a - R_g$ in the presence of oxidizable (ox.) gases, while the form $\Delta R = R_g - R_a$ applies for reducible (red.) gases. R_a and R_g indicate the resistance in air and in the presence of gas, respectively. Highly porous and permeable shell layers are advantageous for the complete electron depletion and effective gas diffusion, respectively, thus yielding high sensing performance in terms of short recovery times and low detection limits [70–73].

An efficient sensing with hierarchical $WO_3 \cdot 0.33H_2O$ nanocolumns was demonstrated by Perfecto et.al. [81], whose

Table 1 Room-temperature gas-sensing properties of metal-oxide-based nanostructures

Materials	Structure	Gas	Concentration	Sensor response or Sensitivity	Response time
SnO_2 [74]	Nanocrystalline tubes	NOx	9.7 ppb	16.1 (ox.)	20 s
SnO_2 [75]	Nanowires	CO	20 ppm	4 (red.)	-
SnO_2 [76]	Thin film	NH_3	50 ppm	6.94 (red.)	175 s
CuO [77]	Nanosheets	H_2S	200 ppb	5.01 (red.)	400 s
CuO-MnO_2 [78]	Nanocomposites	NH_3	100 ppm	135 (red.)	120 s
NiO [79]	Nanowire	NH_3	50 ppm	0.19 (red.)	36 s
Na:ZnO [80]	Nanoflowers	Acetone	100 ppm	2.16 (red.)	-
WO_3 [81]	Nanocolumns	Isopropanol	100 ppm	3 (red.)	53 s
In_2O_3 [82]	Nanocrystals	NOx	970 ppb	1.9 (ox.)	45 s
$W_{18}O_4$ [83]	Nanowires	H_2	25 ppm	0.18 (red.)	-
$LaFeO_3$ [84]	Nanocubes	NO_2	1 ppm	0.29 (ox.)	24 s
Co_3O_4 [85]	Quasi-spherical holes	NH_3	100 ppm	1.46 (red.)	2 s
CuO/SnO_2 [86]	Nanorods	H_2S	ppm	- (red.)	750 s
NiO/WO_3 [87]	Nanoplates	NO_2	30 ppm	4.8 (ox.)	2.5 s
V_2O_5/SnO_2 [88]	Nanowires	Ethanol	100 ppm	14 (red.)	-

sensing results are summarized in Fig. 2. The smooth, uniform columns with hierarchically assembled structures in the FESEM (Field Emission Scanning Electron Microscope) image in Fig. 2a were obtained with a microwave-assisted hydrothermal (MAH) process combined with ultrasonic spray nozzle (USN) methods. The changes in resistance and sensor response are measured by applying a bias voltage of 2V at room temperature with a static gas sensing method as shown in Fig. 2b and it shows the typical p-type behavior, as the resistance increased with increasing isopropanol concentration. The $WO_3 \cdot 0.33H_2O$ gas sensors exhibited fast response (~82 s) and recovery time (~ 260 s) and excellent sensor response (3.4) in a controlled humidity environment (55%), which should be attributed to the high surface area of the nanostructures. Figure 2c displays isopropanol response as a function of gas concentration. The sensor response changed from 1.1 to 6.7 for 1 to 200 ppm isopropanol, confirming the excellent sensing performance of the material. Moreover, a p-type behavior of the material observed after exposure to isopropanol. The gas sensing mechanism at room temperature has been explained as the electronic conduction in an energy-band model and oxygen-vacancy model [81]. When the sensor is exposed to air, oxygen and water molecules are adsorbed on the surface to create a p-type inversion layer at room temperature. As temperature increases, the surface of the sensor becomes intrinsic first due to desorption of water and oxygen molecules, and becomes n-type as the surface gets depleted at high temperature due to further desorption. Additionally, the reverse behavior of p-type gas sensing is also observed. When the sensor is exposed to isopropanol, negative charges were trapped on the surface with decreased oxygen ionic species and the electronic potential decreases with respect to the holes to form an inverse layer as oxygen vacancies. As a result, hole concentration increases and causes the band bending, resulting in the p-type gas sensing response. Details of gas sensing mechanisms for n-type and p-type metal oxides are given in [89].

Fe_2O_3 nanostructures used as sensing materials for room-temperature gas sensors include single Fe_2O_3 nanowires (Fe_2O_3 NWs) fabricated by oxidation of metallic Fe microparticles in ambient air [83]. Fe_2O_3 NWs such as those in Fig. 3a were transferred to a SiO_2/Si substrate with prepatterned Au/Cr electrodes (see Fig. 3b), and connected by Pt contacts at both ends of NWs (Fig. 3c). Detection with the iron oxide sensors was made with the two-probe DC method for four reducible gases at room temperature with controlled humidity (RH 30%). The sensor response increased with decreasing diameter of NW, as shown in Fig. 3d, owing to the larger surface area and fast adsorption-desorption process. Figure 3e, f indicate that the sensor was more selective for

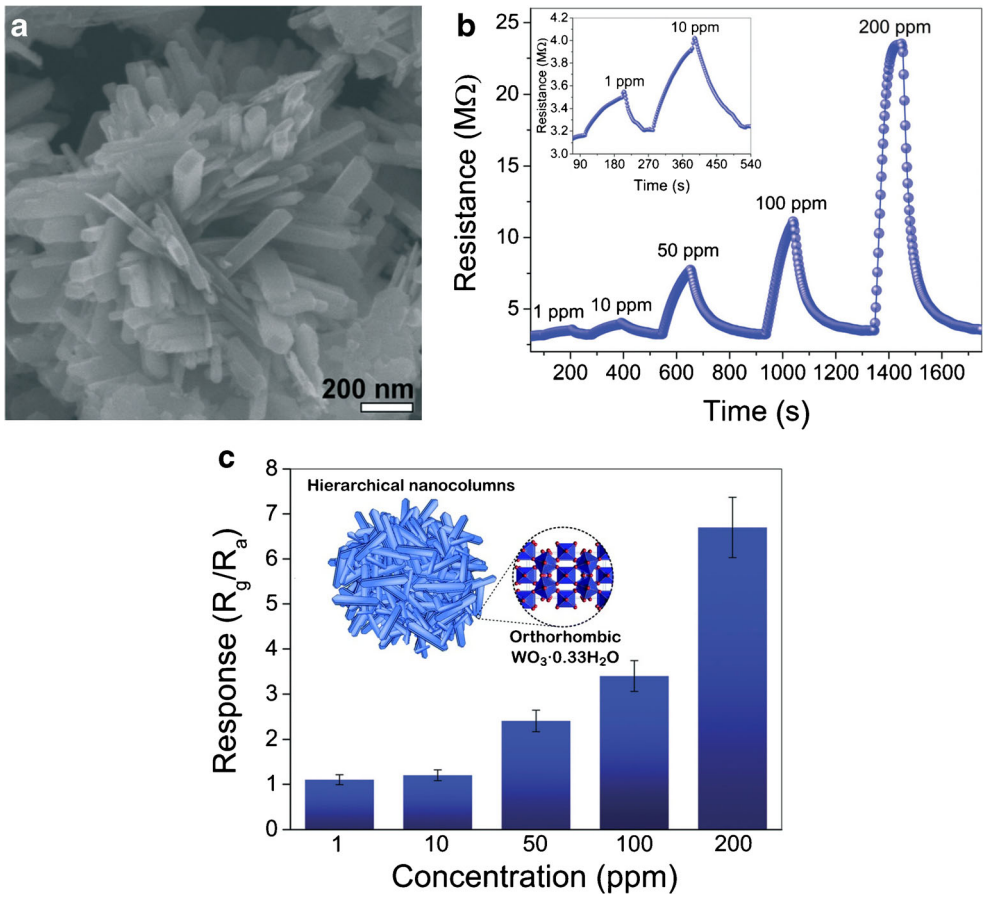

Fig. 2 **a** FESEM and **b** Change in resistance after isopropanol exposure in the concentration range of 1–200 ppm. The inset shows the amplification of the sensor signal for 1 and 10 ppm. **c** chemiresistive sensor responses to isopropanol in the concentration range of 1–200 ppm for $WO_3 \cdot 0.33H_2O$-USN-MAH. Reprint with permission [81], Copyright of The Royal Society of Chemistry

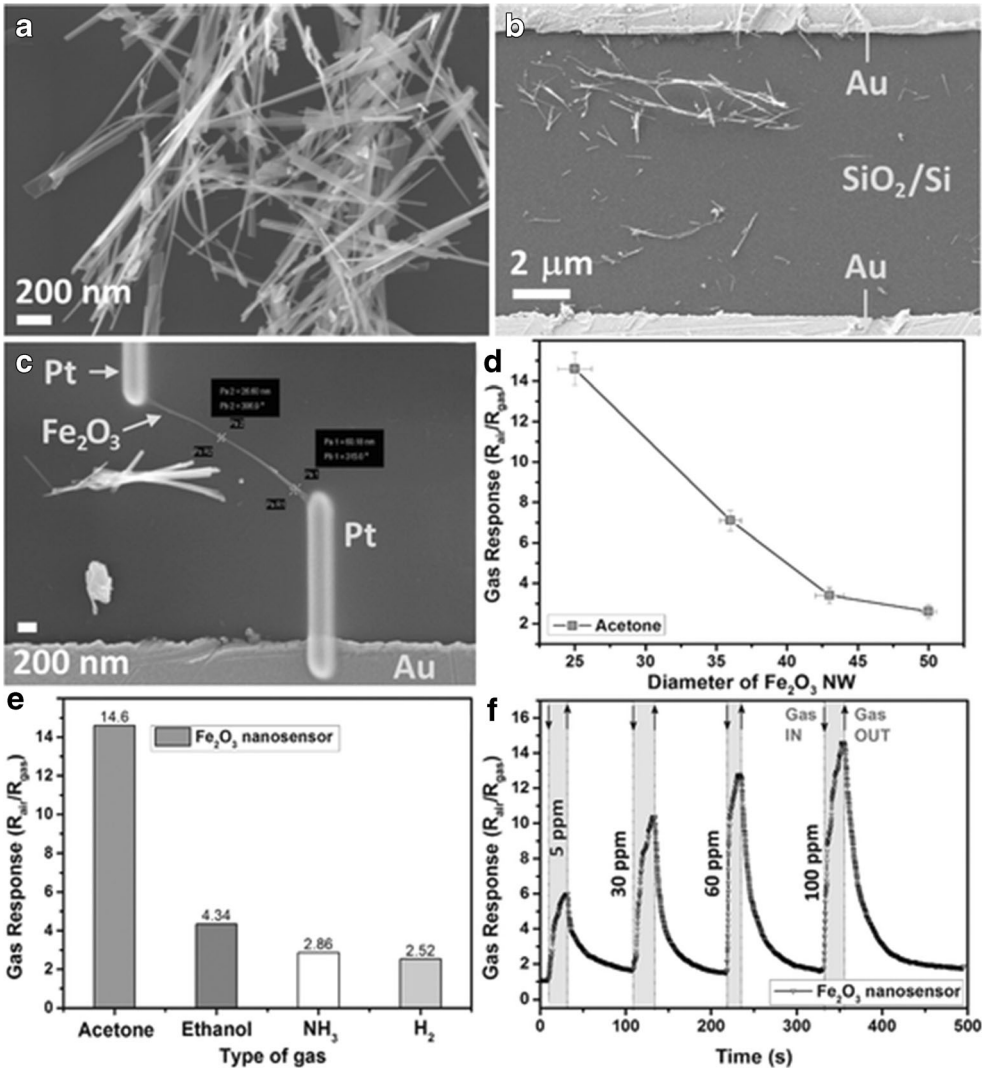

Fig. 3 SEM images of the Fe_2O_3 nanowires **a** on SiO_2/Si substrate after releasing from the initial substrate; and **b** dispersion to a lower concentration. **c** Fabricated nanosensor of single Fe_2O_3 nanowire with D ≈ 25 nm. **d** Sensor response versus diameter of Fe_2O_3 nanowire for 100 ppm acetone vapor. **e** Selectivity histogram of single Fe_2O_3 nanowire with D ≈ 25 nm for different reducible gases. **f** Dynamic chemiresistive gas response for 1–100 ppm acetone vapor at room temperature. Reprint with permission [83], Copyright of Wiley

acetone, and displayed high sensitivity and reproducibility, fast response and recovery times of 16 and 50 s, respectively. The gas sensing mechanism has been discussed with two phenomena: adsorption-desorption of gas molecule on the material surface and band bending. When Fe_2O_3 nanowires surface is exposed to air, chemisorbed oxygen molecules cause the formation of electron-depleted, space charge region. Upon exposure to acetone, electrons are released back to nanowires to reduce the space–charge layer and resistance. A typical feature of such oxide nanostructures exploited in gas sensing are the well-aligned porous structures with high surface area, as discussed in the comprehensive review on hierarchical and hollow oxide nanostructures [90].

The oxide nanostructures discussed here appear to be suitable for room-temperature gas sensing applications with good performances in terms of responses, recovery speed, and long-term stability. Many examples in Table 1 and recent advances in the synthesis of highly porous structures suggest that metal oxide nanostructures are promising candidates for gas sensing at room temperature. In addition to large active surface areas, well-aligned porous structures also allow smooth gas penetration for gas adsorption and desorption processes. However, humidity and gas selectivity are two major challenges for room temperature gas sensing by metal oxide nanostructures. Without heating up the sensing element, H_2O molecules can interfere and compete with oxygen molecules to decrease the sensing responses [91, 92] and a variety of reactions from various gases can occur at room temperature to result in false sensing results. Strategies including surface modifications, doping, ultraviolet (UV) or visible light illuminations have been proposed while further investigations and innovations are needed to address these challenges.

Graphene and its derivatives for gas sensing

Graphene and derivatives such as graphene oxide and reduced graphene oxide have been the most studied carbon materials over the last decade, including for chemical gas sensors

[93–99]. They are suitable for gas sensing owing to their enhanced electron transport properties, efficient adsorption of gas molecules and good signal-to-noise ratio [100, 101]. For the use in gas sensors, graphene has been synthesized via top down and bottom up techniques, including chemical vapor deposition (CVD) [102], exfoliation–intercalation–expansion of graphite [103], arc-discharge techniques [104], epitaxial growth [105], and chemical or thermal reduction of graphene oxide [106]. In the mass production of large-area single layer graphene (SLG) sheets, the CVD growth technique has been preferred because it provides large detection area and controlled sensor fabrication [107, 108]. The very first graphene based gas sensor was reported by Schedin et al. [93] and had micromechanically exfoliated graphene with sub-ppb (part per billion) detection of gas molecules. The main drawback of this sensor was the long recovery time which indicates that at room temperature gas molecules are strongly attached to graphene. It is possible to achieve complete recovery within a shorter time by UV illumination or external heating. In 2012, Yavari et al. [109] demonstrated room temperature detection of NO_2 (100 parts-per-billion (ppb)) and NH_3 (~500 ppb) with graphene films synthesized by CVD. The performance was superior to commercially available NO_2 and NH_3 detectors, and the complete recovery was reached via the joule-heating method to desorb gas molecules.

The 2D nature of graphene provides mechanical flexibility, and various works explored the possibility of operating a graphene FET on a flexible substrate [110–112], especially for wearable applications. The graphene FET transferred on a flexible substrate [113] depicted in Fig. 4a, b was used for gas sensing under various DC gate biases. The graphene FET with a polymeric dielectric film was first deposited on a rigid wafer before being transferred onto a polyimide substrate. A key factor limiting the applications of graphene FET gas sensors is the selectivity issue. Figure 4c, d show that four gases can be clearly distinguished with a single graphene FET upon extracting a linear factor by tracking the change of field effect mobility and Dirac Point voltage. The y-axis represents the reverse of the field effect mobility of graphene (the delta symbol denotes the "change"), having therefore the unit of [Vs/cm^2]) and the x-axis indicates the Dirac Point voltage [114]. Another recent advance in improving graphene FET sensor performance is to accelerate the poor recovery speed at room temperature, which is typically from hundreds to thousands of seconds [115]. The recovery speed can be boosted by 10 times when graphene FET is operated in an AC scheme (AC phase measurements), as compared to the conventional DC scheme (DC resistance measurements) [116]. Figure 4e shows the sensitive distance of AC is far enough to reach the weakly adsorbed gas molecules for a quicker desorption process in comparison with DC sensing schemes where the sensing distance is limited by the charge transfer RC time constant as modeled in Fig. 4f. Figure 4g, h compare the drift-free sensing results of saturated ethanol vapor by using AC sensing scheme

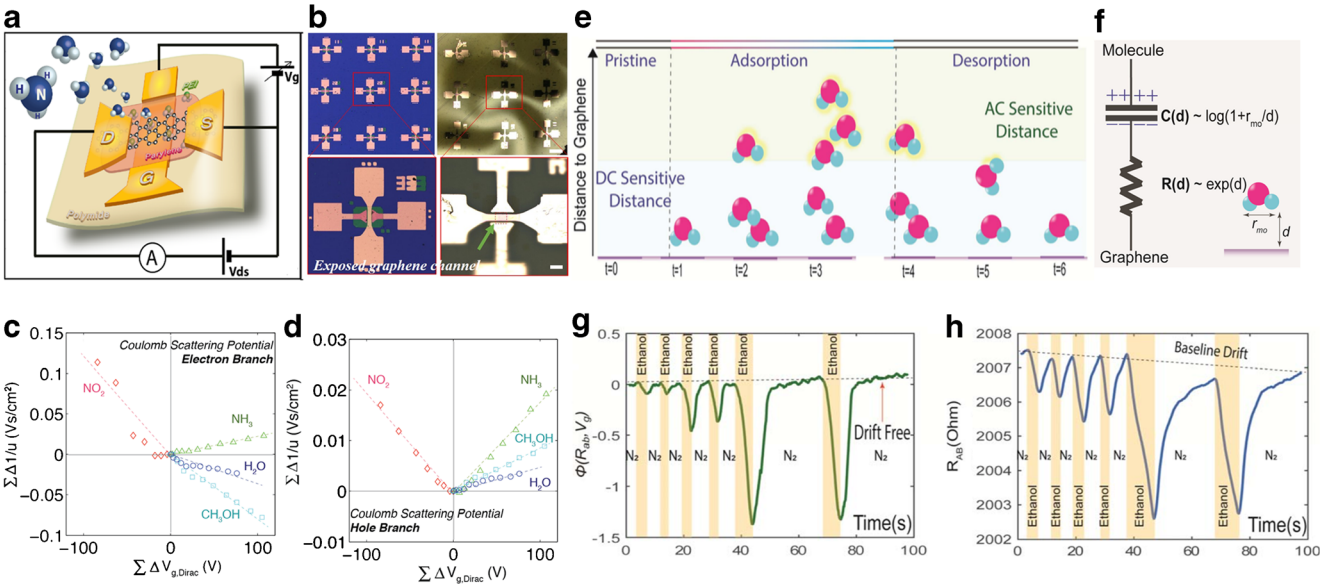

Fig. 4 **a** Schematic diagram of the flexible graphene FET for gas sensing. **b** An array of 3x3 devices before polyimide coating and after polyimide coating and separation on a flexible substrate (scale bar 70 μm). Also shown are magnified views of the corresponding single transistor on the bottom (scale bar 7 μm). Linear factor measured for four types of gases on a single graphene FET in electron **c** branch and **d** hole branch, showing the selectivity. **e** Illustration of the AC sensing scheme which is more effective to detect weakly adsorbed gases (faster desorption) away from the graphene surface than DC sensing. **f** The RC model of the charge transfers pathway between adsorbed gas and graphene with a distance "d." The experimental results of the **g** AC sensing signal and **h** DC sensing signal measured simultaneously on a graphene FET under 6 cycles of saturated ethanol vapor injections. Reprint with permission [113, 114, 116], Copyright of IEEE

(Fig. 4g) and drifted sensing results measured simultaneously using the DC sensing scheme (Fig. 4h), showing the improved sensing recovery speed of graphene FET.

Noble metals have proven their potential to improve sensing performance, but they are expensive [117–119]. Metal oxides have therefore been used in gas sensors, which may include nanocomposites with graphene [120–124]. Song and co-workers reported the one-step colloidal synthesis of SnO_2 quantum wire/reduced graphene oxide nanocomposites as selective gas sensors for H_2S with detection in the 10-100 ppm range with fast response/recovery time (2/292 s), better sensor response (~33) as compared to pure reduced graphene oxide [125]. The HRTEM (High-resolution transmission electron microscopy) image in Fig. 5a shows well dispersed, crystalline SnO_2/rGO nanocomposites, while Fig. 5b illustrates the fast response at room temperature for a wide concentration range. The histogram in Fig. 5c confirms the high selectivity for H_2S, in comparison with NO_2, SO_2, NH_3 and ethanol vapor. Figure 5d displays the response curves of gas sensors based on pristine rGO, pure SnO_2 quantum wires (8 h) and SnO_2/rGO nanocomposites (8 h). The gas sensing mechanism is related to the formation of Schottky junctions between graphene and metal oxides as the Schottky barrier determined by the work-function difference between metals and semiconductors is affected by adsorbed chemical species. At the SnO_2/rGO junction, electrons are moving from the smaller work function of SnO_2 to rGO to balance the Fermi level. The H_2S gas molecules provide electrons to increase the potential barrier for electrons to flow from SnO_2 to rGO, which results in decrease in resistance.

Table 2 illustrates the recent advances on room-temperature gas sensors made with scalable graphene fabrications, which are highly selective and sensitive to target gases. It is significant that these sensors display efficient recovery speed without the assistance of UV/IR light illuminations or thermal effects. A critical analysis of the literature indicates that graphene composites decorated with metals and metal oxides yield higher performance in room-temperature gas sensing than pristine graphene. The main strength of graphene-based sensors is the high sensitivity for a range of gases, reaching ppm (parts per million) levels. The drawbacks are associated with poor specificity in many cases, slow recovery time, and potential high cost. As a result, graphene-based materials seem not as efficient for room-temperature gas sensing as

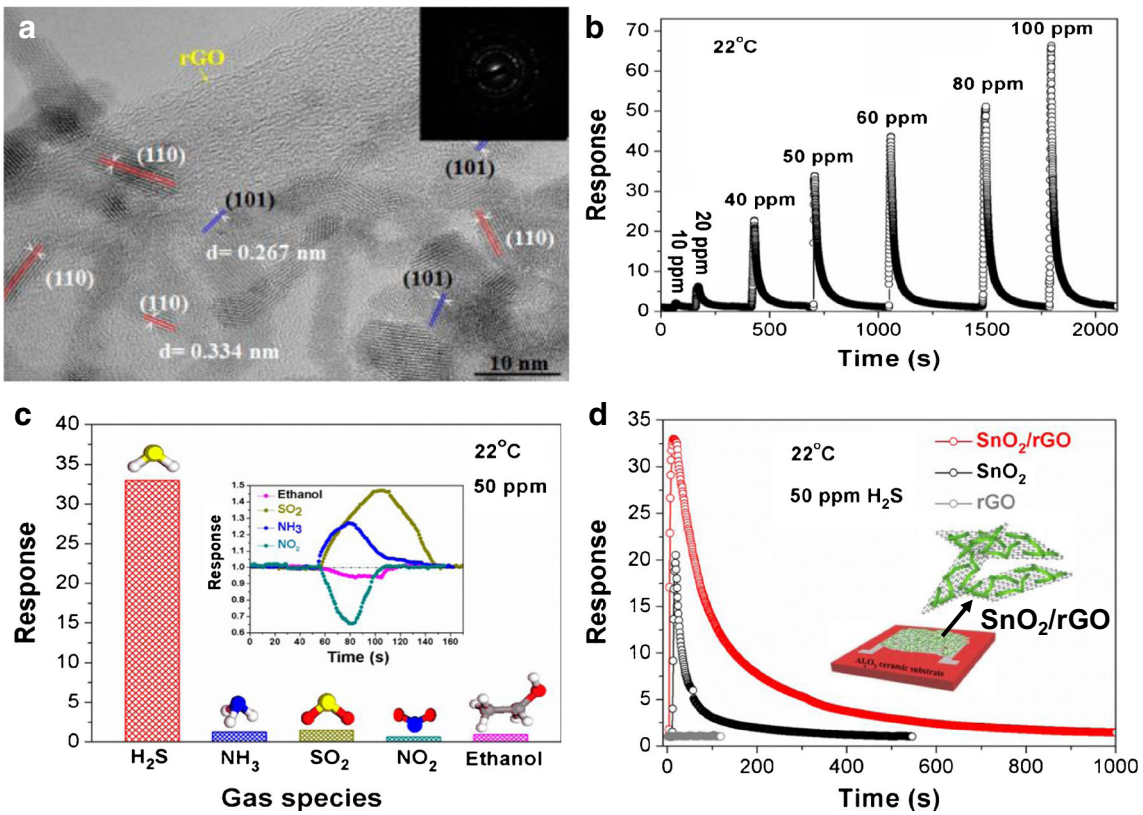

Fig. 5 **a** High-resolution transmission electron microscopy (HRTEM) image and selected area electron diffraction (SAED) pattern of the SnO_2/rGO nanocomposites synthesized at 180 °C for 8 h. **b** Chemiresitive response curves toward different concentrations of H_2S. **c** Selectivity of the optimal gas sensor employing SnO_2/rGO nanocomposites. **d** Response curves with the sensor response defined as the ratio of R_a to R_g, where R_a is the resistance in the air and R_g is the resistance in the presence of a target gas. The sensors were made of pristine rGO, SnO_2 quantum wires (8 h) and SnO_2/rGO nanocomposites (8 h). Reprint with permission [125]. Copyright of American Chemical Society

Table 2 Room-temperature gas-sensing properties of graphene-based nanostructures

Materials	Structure	Gas	Concentration	Sensor response or Sensitivity	Response time
Graphene [95]	Sheet	CO_2	100 ppm	26 (ox.)	8 s
Reduced Graphene Oxide [126]	Flakes	NH_3	800 ppm	11 (red.)	540 s
Reduced graphene oxide [127]	Nanosheets	SO_2	5 ppm	5.93 (ox.)	122 s
Ag-Sulfonated graphene [128]	film	NO_2	50 ppm	45 (ox.)	12 s
Graphene/SnO_2 [129]	film	Acetone	10 ppm	2.19 (red.)	107 s
rGO/TiO_2 [130]	Hybrid	Methanol	10 ppm	24.66 (red.)	18 s
rGO/CuO [131]	Nanosheets	Formaldehyde	100 ppm	7.07 (red.)	108 s
rGO/ZnO [132]	Mesoporous	NO_2	1 ppm	119 (ox.)	75 s
rGO/CuO [133]	Composites	CO	1 ppm	2.56 (red.)	70 s
rGO-WO_3 [134]	Nanosheet	NO_2	5 ppm	0.7 (ox.)	600 s
Co_3O_4-rGO [135]	Nanosheets	NO_2	60 ppm	0.8 (ox.)	-
NiO-rGO [136]	Nanosheets	NO_2	15 ppm	1.1 (ox.)	-
In_2O_3-rGO [137]	Nanosheets	NO_2	30 ppm	8.25 (ox.)	240 s

those based on the oxide nanostructures at the present time. However, high sensitivity and possible optimizations together with new innovations, and low-cost, large area manufacturing with a wide variety of graphene composites could make the graphene-based room temperature gas sensing promising in the future.

Gas sensors based on 2D transition metal dichalcogenides (TMDs)

Transition metal dichalcogenides (TMDs) are materials with the formula of MX_2, where M refers to a transition metal element such as Mo, W, Hf, Ti, Zr, V, Nb, Ta, Re, etc. and X represents a chalcogen (S, Se or Te) [138–140]. Two-dimensional (2D) structures of TMDs have attracted renewed interest due to their superior molecular sensing capability, unique physical and chemical properties, including semiconducting property and high surface-to-volume ratio [141–145]. These 2D layered materials such as MoS_2, WS_2, ReS_2, $MoSe_2$, WSe_2 and $ReSe_2$, with atomically thin-layered structure, are potentially effective sensing materials [46, 146–149]. They may be synthesized with various techniques, including CVD [150], micromechanical exfoliation and liquid exfoliation [151]. The latter is the most often used since it is suitable for large-scale devices in electronics, optoelectronics and gas sensing. These 2D TMDs have been amenable for room- temperature sensing but recovery was poor, while a high performance was achieved with thermal assistance or UV illumination but then there is the issue of energy consumption [46, 152].

Some of the room-temperature gas sensors made with these atomically thin-layered 2D materials are based on field-effect transistors (FET), which are difficult to fabricate, thereby limiting the throughput of sensor production. Li et.al. [54] reported single- and multilayer MoS_2 film-based FET for NO sensing at room temperature. FET devices were fabricated with exfoliated one to four layer of n-type MoS_2 films, but practical applications were hindered because of a poor response toward NO gas and slow recovery, which were worse than those of previously demonstrated sensors based on single-layer MoS_2 transistors. 3D assemblies of these 2D materials provide more surface area per footprint with a reproducible, scalable synthesis process as compared to single and few layer MoS_2. Cho et.al. [153] produced MoS_2 nanofilms by CVD capable of detecting NO_2 at room temperature at ppb level (120-1200 ppb), but the recovery time was long. For full gas desorption, MoS_2 was heated to 100 °C but the sensitivity was lowered. To overcome this difficulty with improved sensitivity, metal dichalcogenide surfaces are being functionalized with sensitizers, dopants and metal oxides. Some recent advances of MoS_2 and WS_2 based gas sensors for room-temperature operation are summarized in Table 3.

Li et al. [165] investigated room temperature chemiresistive ammonia sensing for 2D WS_2 nanoflakes which showed excellent sensitivity (1-100ppm) and good selectivity as compared to other target gases. Figure 6a shows the layered spherical flake morphology with diameter of 1–4 micrometers and thickness around 110 nm. The dynamic response curve as a function of time at room temperature and relative humidity for WS_2 nanoflakes are shown in Fig. 6b. The resistance of WS_2 increased upon exposure to ammonia indicating a "p-type" behavior since ammonia is a reducible gas. The response and recovery time was ~120 s and ~150 s, respectively. The sensor response increased with increasing relative humidity up to 73% due to the hydroxylation reaction on the WS_2 surface, but saturation was observed if the humidity was increased further to 99% (Fig. 6c).

Other metal dichalcogenides such as $MoSe_2$ and SnS_2 [159, 166] have also shown promising gas sensing properties. Late et al. [167] studied the gas sensing properties of single layer $MoSe_2$ prepared by mechanical exfoliation, whose SEM

Table 3 Room-temperature gas-sensing properties of 2D nanostructures

Materials	Structure	Gas	Concentration	Sensor response or Sensitivity	Response time
MoS_2 [154]	Thin films	NH_3	300 ppb	4.2 (SNR*) (red.)	15 s
MoS_2 [155]	Thin films	NO_2	10 ppm	~23 (ox.)	-
$MoSe_2$ [156]	Thin Film	NO_2	300 ppm	1907 (ox.)	1200 s <
WS_2 [157]	Nanosheets	NO_2	25 ppm	8.7 (ox.)	-
Ag-WS_2 [157]	Nanosheets	NO_2	25 ppm	58 (ox.)	-
WS_2-Pd [158]	Thin film	H_2	50,000 ppm	0.78 (red.)	119 s
SnS_2 [159]	Flower-shaped	NH_3	5 ppm	21.6 (red.)	~50 s
Ni-MoS_2 [160]	Nanoflowers	SO_2	5 ppm	7.4 (ox.)	50 s
WS_2-TiO_2 [161]	Nanohybrids	NH_3	250 ppm	43.72 (red.)	200 s
MoS_2/ZnO [162]	Nanocomposites	NH_3	50 ppm	46.2 (red.)	10 s
MoS_2/SnO_2 [163]	Nanosheet	NO_2	10 ppm	28 (ox.)	408 s
MoS_2 –rGO [164]	Hybrid	Formaldehyde	10 ppm	~2.8 (red.)	73 s
Pd-SnO_2/MoS_2 [165]	Composite	Hydrogen	500 ppm	~5 (red.)	23 s

SNR* Signal to Noise Ratio

image and picture are shown in Fig. 7a. The performance of the exfoliated single layer $MoSe_2$ was investigated by exposing the sensor to various concentrations (50-500 ppm) of ammonia (Fig. 7b, c). The single $MoSe_2$ layer showed high sensitivity (~1200) for 500 ppm of ammonia with fast response (~150 s) and recovery (~9 min.), which is lower than that reported for single-layer MoS_2. Generally, strong adhesion of gas molecules to the sensing material favors sensitivity but it also makes it more difficult to remove the sensed materials, which is the reason for the slow recovery time of 2D material-based gas sensors. The gas sensing mechanism of 2D TMDs is based on the charge transfer process. In this case, when ammonia molecules are adsorbed onto $MoSe_2$ surfaces, lone-pair electron acts as an electron donor, and transfers its

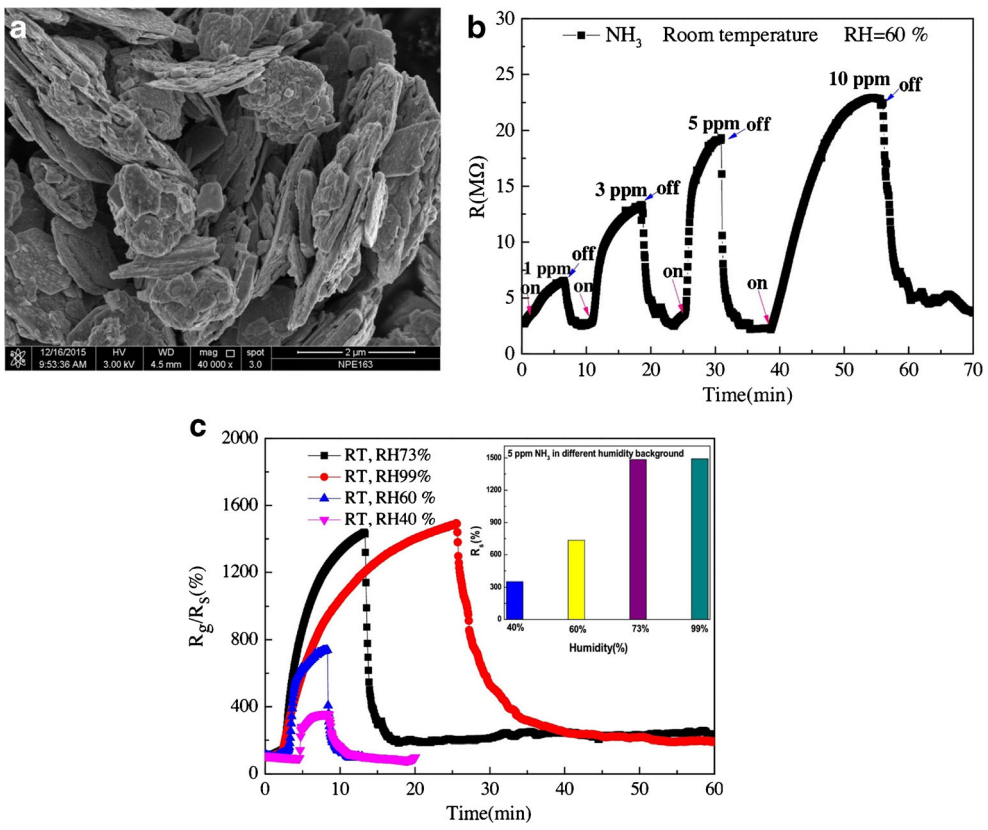

Fig. 6 **a** SEM image of WS_2 nanoflakes. **b** Dynamic chemiresistive response curve of the sensor made with WS_2 nanoflakes as a function of time to 1–10 ppm ammonia. **c** Influence of relative humidity in the air background on the WS_2 nanoflake based sensor response to 5 ppm ammonia at room temperature. Reprint with permission [165], Copyright of Elsevier

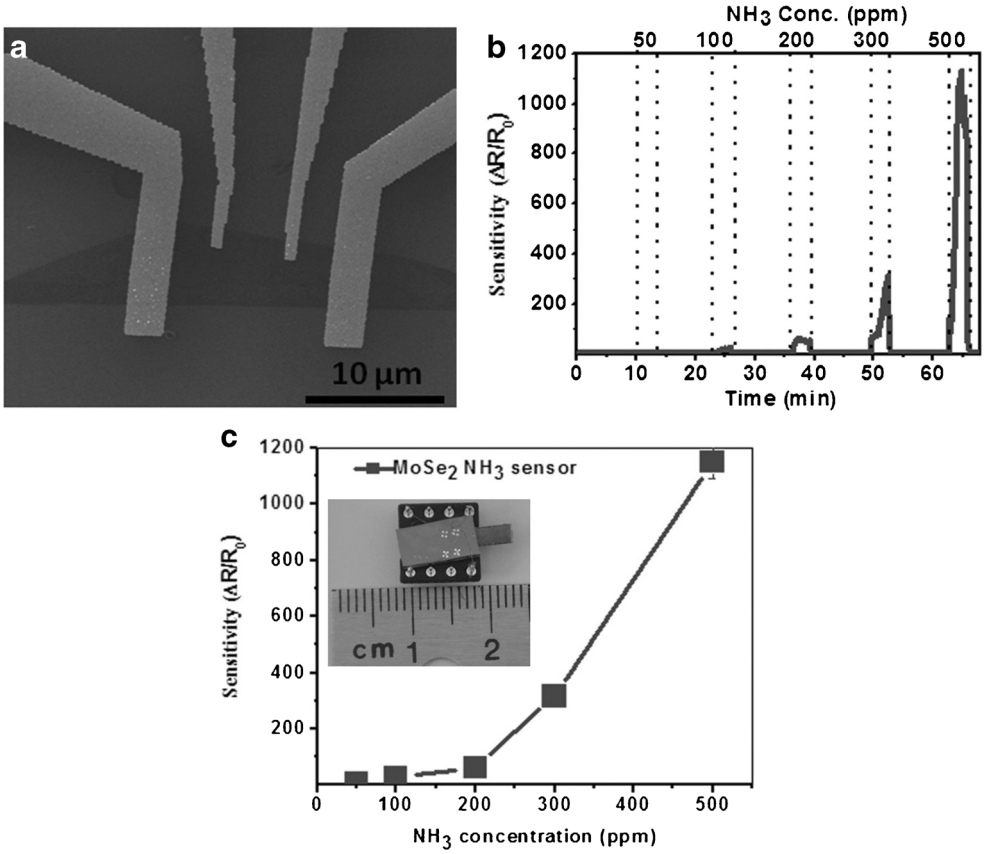

Fig. 7 Single-layer $MoSe_2$ **a** SEM image, **b** ammonia sensitivity ($\left|\frac{\Delta R}{R_0}\right| \times 100$, where $\Delta R = R_g - R_0$, while R_0 and R_g indicate the resistance in air and in the presence of gas, respectively) as function of gas concentration, **c** linear plot of sensitivity of $MoSe_2$ gas sensor device as a function of ammonia gas concentration (ppm). Reprint with permission [167]. Copyright of AIP Publishing LLC

electron to the conduction band of $MoSe_2$. Such a charge transfer process induces an increased electron concentration and electrical conductivity.

In spite of the promising results as illustrated above, improvements in 2D TMDs are needed to reach high sensitivity, selectivity, and stability. Specifically, an important limitation of 2D TMDs for room-temperature gas sensing is the slow recovery time owing to the slow gas desorption process. As of now, these materials appear to be inferior in terms of the sensing performances when compared with those made of metal oxide nanostructures but display similar responses as those made of pristine graphene.

Conclusion and future prospects

The fabrication of gas sensors has undergone a revolutionary transition from powder-based thick films to thin

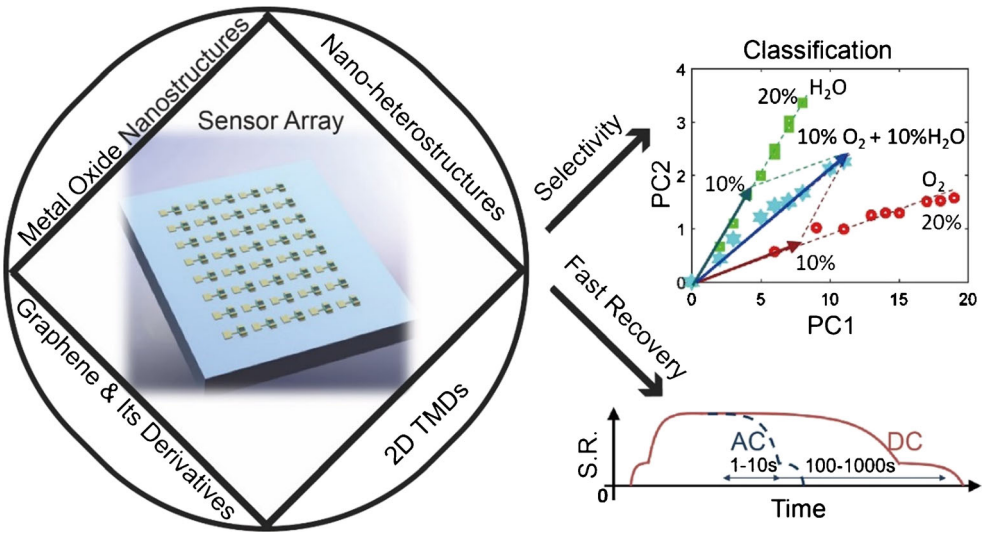

Fig. 8 The concept of selective sensing and fast recovery by using an arrays of gas sensors combining different sensing materials and/or schemes to offer multi-variable responses, and thereby provide selectivity via data-assisted pattern recognition and machine-learning schemes and fast recovery by using the AC sensing scheme [171]

films produced by physical or chemical vapor deposition. These methods enable finer control over materials microstructures such as grain size and boundary, and may allow for fabrication of porous structures that are suitable for gas sensing. In a survey of the literature, three classes were identified of nanotech-based materials with porous morphology and amenable to room-temperature gas sensing. Oxide nanostructures, graphene composites and 2D transition metal dichalcogenides (TMDs) have indeed been proven as suitable for instantaneous detection of toxic and hazardous gases and real-time gas monitoring under controlled humidity. There are important limitations to these materials though, mostly associated with the need to improve selectivity and stability. Furthermore, the gas sensing mechanism is still not well established for graphene and 2D TMDs. It is our belief that these limitations may be overcome in the near future via surface functionalization and the design of heterostructures exploiting the wide variety of nanomaterials. In addition to the strategies discussed in the review, several other directions are being exploited. For example, improvements in the recovery speed can be obtained by introducing the AC test method [168]. The AC test offers phase change responses which are only sensitive to the weak adsorption of gas molecules above a distance to the graphene surface for fast gas adsorption and desorption processes, while the conventional DC resistance results are sensitive to the strong adsorption and desorption process close to the sensing material surface. Arrays of gas sensors combining different sensing materials and/or schemes may offer multi-variable responses, and thereby provide selectivity via data-assisted pattern recognition and machine-learning schemes [169–171]. For example, an array of sensors with different sensing materials and/or schemes such as metal oxide nanostructures, nanoheterostructures, graphene and its derivatives, and 2D TMDs as shown in Fig. 8 could respond to individual vapors or vapor mixtures with distinguishable response patterns - much like the way the mammalian olfactory system to produce diagnostic patterns. This approach may address the key gas sensing problems in selectivity and fast recovery speed to meet the requirements in practical applications in a multi-gas environment.

Acknowledgements This work had financial support in part from FAPESP (2014/23546-1, 2016/23474-6), in part from Midea Group, and in part by a National Science Foundation grant (ECCS 1711227). The authors are also thankful to Berkeley Sensor and Actuator Centre (BSAC). Professor Liwei Lin is a core-principal investigator of the Tsinghua-Berkeley Shenzhen Institute (TBSI) and acknowledge the funding support of TBSI.

Compliance with ethical standards The authors declare that they have no competing interests.

References

1. Dieter K (2001) Function and applications of gas sensors. J Phys D Appl Phys 34(19):R125
2. Fine GF, Cavanagh LM, Afonja A, Binions R (2010) Metal Oxide Semi-Conductor Gas Sensors in Environmental Monitoring. Sensors (Basel, Switzerland) 10(6):5469–5502. https://doi.org/10.3390/s100605469
3. Zhang J, Qin Z, Zeng D, Xie C (2017) Metal-oxide-semiconductor based gas sensors: screening, preparation, and integration. Phys Chem Chem Phys 19(9):6313–6329. https://doi.org/10.1039/c6cp07799d
4. Varghese SS, Lonkar S, Singh KK, Swaminathan S, Abdala A (2015) Recent advances in graphene based gas sensors. Sensors Actuators B Chem 218(Supplement C):160–183. https://doi.org/10.1016/j.snb.2015.04.062
5. Gusain A, Joshi NJ, Varde PV, Aswal DK (2017) Flexible NO gas sensor based on conducting polymer poly[N-9′-heptadecanyl-2,7-carbazole-alt-5,5-(4′,7′-di-2-thienyl-2′,1′,3′-benzothiadiazole)] (PCDTBT). Sensors Actuators B Chem 239:734–745. https://doi.org/10.1016/j.snb.2016.07.176
6. Joshi N, Saxena V, Singh A, Koiry SP, Debnath AK, Chehimi MM, Aswal DK, Gupta SK (2014) Flexible H2S sensor based on gold modified polycarbazole films. Sensors Actuators B Chem 200(Supplement C):227–234. https://doi.org/10.1016/j.snb.2014.04.041
7. Yoriya S, Prakasam HE, Varghese OK, Shankar K, Paulose M, Mor GK, Latempa TJ, Grimes CA (2006) Initial Studies on the Hydrogen Gas Sensing Properties of Highly-Ordered High Aspect Ratio TiO2 Nanotube-Arrays 20 m to 222 m in Length. Sens Lett 4(3):334–339. https://doi.org/10.1166/sl.2006.042
8. Singh A, Kumar A, Kumar A, Samanta S, Joshi N, Balouria V, Debnath AK, Prasad R, Salmi Z, Chehimi MM, Aswal DK, Gupta SK (2013) Bending stress induced improved chemiresistive gas sensing characteristics of flexible cobalt-phthalocyanine thin films. Appl Phys Lett 102(13):132107. https://doi.org/10.1063/1.4800446
9. Ramgir N, Datta N, Kaur M, Kailasaganapathi S, Debnath AK, Aswal DK, Gupta SK (2013) Metal oxide nanowires for chemiresistive gas sensors: Issues, challenges and prospects. Colloids Surf A Physicochem Eng Asp 439:101–116. https://doi.org/10.1016/j.colsurfa.2013.02.029
10. Shaik M, Rao VK, Gupta M, Murthy KSRC, Jain R (2016) Chemiresistive gas sensor for the sensitive detection of nitrogen dioxide based on nitrogen doped graphene nanosheets. RSC Adv 6(2):1527–1534. https://doi.org/10.1039/c5ra21184k
11. Mirica KA, Azzarelli JM, Weis JG, Schnorr JM, Swager TM (2013) Rapid prototyping of carbon-based chemiresistive gas sensors on paper. Proc Natl Acad Sci 110(35):E3265–E3270. https://doi.org/10.1073/pnas.1307251110
12. Joshi N, da Silva LF, Jadhav H, M'Peko J-C, Millan Torres BB, Aguir K, Mastelaro VR, Oliveira ON (2016) One-step approach for preparing ozone gas sensors based on hierarchical NiCo2O4 structures. RSC Adv 6(95):92655–92662. https://doi.org/10.1039/c6ra18384k
13. Kumar A, Joshi N, Samanta S, Singh A, Debnath AK, Chauhan AK, Roy M, Prasad R, Roy K, Chehimi MM, Aswal DK, Gupta SK (2015) Room temperature detection of H2S by flexible gold–cobalt phthalocyanine heterojunction thin films. Sensors Actuators B Chem 206(Supplement C):653–662. https://doi.org/10.1016/j.snb.2014.09.074
14. Balouria V, Samanta S, Singh A, Debnath AK, Mahajan A, Bedi RK, Aswal DK, Gupta SK (2013) Chemiresistive gas sensing properties of nanocrystalline Co3O4 thin films. Sensors

Actuators B Chem 176(Supplement C):38–45. https://doi.org/10.1016/j.snb.2012.08.064

15. Joshi N, Shimizu FM, Awan IT, M'Peko JC, Mastelaro VR, Oliveira ON, Da Silva LF (2016) Ozone sensing properties of nickel phthalocyanine:ZnO nanorod heterostructures. In: IEEE Sensors, Orlando, USA. In Proceedings of IEEE Sensors, pp 1-3. doi:https://doi.org/10.1109/ICSENS.2016.7808407
16. Seiyama T, Kato A, Fujiishi K, Nagatani M (1962) A New Detector for Gaseous Components Using Semiconductive Thin Films. Anal Chem 34(11):1502–1503. https://doi.org/10.1021/ac60191a001
17. Rane YN, Shende DA, Raghuwanshi MG, Ghule AV, Patil VL, Patil PS, Gosavi SR, Deshpande NG (2017) Synthesis of flower shaped ZnO thin films for resistive sensing of NO2 gas. Microchim Acta 184(7):2455–2463. https://doi.org/10.1007/s00604-017-2271-7
18. Yadav AA, Lokhande VC, Bulakhe RN, Lokhande CD (2017) Amperometric CO2 gas sensor based on interconnected web-like nanoparticles of La2O3 synthesized by ultrasonic spray pyrolysis. Microchim Acta 184(10):3713–3720. https://doi.org/10.1007/s00604-017-2364-3
19. Ponnusamy D, Prasad AK, Madanagurusamy S (2016) CdO-TiO2 nanocomposite thin films for resistive hydrogen sensing. Microchim Acta 183(1):311–317. https://doi.org/10.1007/s00604-015-1653-y
20. Tian J, Yang G, Jiang D, Su F, Zhang Z (2016) A hybrid material consisting of bulk-reduced TiO2, graphene oxide and polyaniline for resistance based sensing of gaseous ammonia at room temperature. Microchimica Acta 183(11):2871–2878. https://doi.org/10.1007/s00604-016-1912-6
21. Rahman MM, Balkhoyor HB, Asiri AM, Marwani HM (2016) A gold electrode modified with silver oxide nanoparticle decorated carbon nanotubes for electrochemical sensing of dissolved ammonia. Microchim Acta 183(5):1677–1685. https://doi.org/10.1007/s00604-016-1797-4
22. Tamvakos A, Calestani D, Tamvakos D, Mosca R, Pullini D, Pruna A (2015) Effect of grain-size on the ethanol vapor sensing properties of room-temperature sputtered ZnO thin films. Microchim Acta 182(11):1991–1999. https://doi.org/10.1007/s00604-015-1539-z
23. Hasani A, Dehsari HS, Gavgani JN, Shalamzari EK, Salehi A, Afshar Taromi F, Mahyari M (2015) Sensor for volatile organic compounds using an interdigitated gold electrode modified with a nanocomposite made from poly(3,4-ethylenedioxythiophene)-poly(styrenesulfonate) and ultra-large graphene oxide. Microchim Acta 182(7):1551–1559. https://doi.org/10.1007/s00604-015-1487-7
24. Mekki A, Joshi N, Singh A, Salmi Z, Jha P, Decorse P, Lau-Truong S, Mahmoud R, Chehimi MM, Aswal DK, Gupta SK (2014) H2S sensing using in situ photo-polymerized polyaniline–silver nanocomposite films on flexible substrates. Org Electron 15(1):71–81. https://doi.org/10.1016/j.orgel.2013.10.012
25. Bae JS, Yun DH, Park CO, Hwang JS (2001) Improved selectivity of oxide semiconductor type gas sensor using compensating element. Sensors Actuators B Chem 75(3):160–165. https://doi.org/10.1016/S0925-4005(00)00738-3
26. Stankova M, Vilanova X, Calderer J, Llobet E, Brezmes J, Gràcia I, Cané C, Correig X (2006) Sensitivity and selectivity improvement of rf sputtered WO3 microhotplate gas sensors. Sensors Actuators B Chem 113(1):241–248. https://doi.org/10.1016/j.snb.2005.02.056
27. Rigoni F, Tognolini S, Borghetti P, Drera G, Pagliara S, Goldoni A, Sangaletti L (2013) Enhancing the sensitivity of chemiresistor gas sensors based on pristine carbon nanotubes to detect low-ppb ammonia concentrations in the environment. Analyst 138(24):7392–7399. https://doi.org/10.1039/c3an01209c
28. Mortazavi Zanjani SM, Sadeghi MM, Holt M, Chowdhury SF, Tao L, Akinwande D (2016) Enhanced sensitivity of graphene ammonia gas sensors using molecular doping. Appl Phys Lett 108(3):033106. https://doi.org/10.1063/1.4940128
29. Singh A, Salmi Z, Joshi N, Jha P, Kumar A, Lecoq H, Lau S, Chehimi MM, Aswal DK, Gupta SK (2013) Photo-induced synthesis of polypyrrole-silver nanocomposite films on N-(3-trimethoxysilylpropyl)pyrrole-modified biaxially oriented polyethylene terephthalate flexible substrates. RSC Adv 3(16):5506–5523. https://doi.org/10.1039/c3ra22981e
30. Saboor FH, Ueda T, Kamada K, Hyodo T, Mortazavi Y, Khodadadi AA, Shimizu Y (2016) Enhanced NO2 gas sensing performance of bare and Pd-loaded SnO2 thick film sensors under UV-light irradiation at room temperature. Sensors Actuators B Chem 223(Supplement C):429–439. https://doi.org/10.1016/j.snb.2015.09.075
31. Ueda T, Abe H, Kamada K, Bishop SR, Tuller HL, Hyodo T, Shimizu Y (2017) Enhanced sensing response of solid-electrolyte gas sensors to toluene: Role of composite Au/metal oxide sensing electrode. Sensors Actuators B Chem 252(Supplement C):268–276. https://doi.org/10.1016/j.snb.2017.05.172
32. Ponzoni A, Baratto C, Cattabiani N, Falasconi M, Galstyan V, Nunez-Carmona E, Rigoni F, Sberveglieri V, Zambotti G, Zappa D (2017) Metal Oxide Gas Sensors, a Survey of Selectivity Issues Addressed at the SENSOR Lab, Brescia (Italy). Sensors 17(4). https://doi.org/10.3390/s17040714
33. Gessner T, Gottfried K, Hoffmann R, Kaufmann C, Weiss U, Charetdinov E, Hauptmann P, Lucklum R, Zimmermann B, Dietel U, Springer G, Vogel M (2000) Metal oxide gas sensor for high temperature application. Microsyst Technol 6(5):169–174. https://doi.org/10.1007/s005420000048
34. Wang C, Yin L, Zhang L, Xiang D, Gao R (2010) Metal Oxide Gas Sensors: Sensitivity and Influencing Factors. Sensors (Basel, Switzerland) 10(3):2088–2106. https://doi.org/10.3390/s100302088
35. Arbab A, Spetz A, Lundström I (1993) Gas sensors for high temperature operation based on metal oxide silicon carbide (MOSiC) devices. Sensors Actuators B Chem 15(1):19–23. https://doi.org/10.1016/0925-4005(93)85022-3
36. Yoon H (2013) Current Trends in Sensors Based on Conducting Polymer Nanomaterials. Nanomaterials 3(3):524–549. https://doi.org/10.3390/nano3030524
37. Bai H, Shi G (2007) Gas Sensors Based on Conducting Polymers. Sensors (Basel, Switzerland) 7(3):267–307
38. Miasik JJ, Hooper A, Tofield BC (1986) Conducting polymer gas sensors. J Chem Soc Faraday Trans 1 82(4):1117–1126. https://doi.org/10.1039/f19868201117
39. Chen G, Paronyan TM, Pigos EM, Harutyunyan AR (2012) Enhanced gas sensing in pristine carbon nanotubes under continuous ultraviolet light illumination. 2:343. https://doi.org/10.1038/srep00343
40. Majhi SM, Rai P, Yu Y-T (2015) Facile Approach to Synthesize Au@ZnO Core–Shell Nanoparticles and Their Application for Highly Sensitive and Selective Gas Sensors. ACS Appl Mater Interfaces 7(18):9462–9468. https://doi.org/10.1021/acsami.5b00055
41. Tian H, Fan H, Dong G, Ma L, Ma J (2016) NiO/ZnO p-n heterostructures and their gas sensing properties for reduced operating temperature. RSC Adv 6(110):109091–109098. https://doi.org/10.1039/c6ra19520b
42. Schütt F, Postica V, Adelung R, Lupan O (2017) Single and Networked ZnO–CNT Hybrid Tetrapods for Selective Room-Temperature High-Performance Ammonia Sensors. ACS Appl

Mater Interfaces 9(27):23107–23118. https://doi.org/10.1021/acsami.7b03702
43. Mishra YK, Modi G, Cretu V, Postica V, Lupan O, Reimer T, Paulowicz I, Hrkac V, Benecke W, Kienle L, Adelung R (2015) Direct Growth of Freestanding ZnO Tetrapod Networks for Multifunctional Applications in Photocatalysis, UV Photodetection, and Gas Sensing. ACS Appl Mater Interfaces 7(26):14303–14316. https://doi.org/10.1021/acsami.5b02816
44. Lupan O, Postica V, Gröttrup J, Mishra AK, de Leeuw NH, Carreira JFC, Rodrigues J, Ben Sedrine N, Correia MR, Monteiro T, Cretu V, Tiginyanu I, Smazna D, Mishra YK, Adelung R (2017) Hybridization of Zinc Oxide Tetrapods for Selective Gas Sensing Applications. ACS Appl Mater Interfaces 9(4):4084–4099. https://doi.org/10.1021/acsami.6b11337
45. Zhang J, Liu X, Neri G, Pinna N (2016) Nanostructured Materials for Room-Temperature Gas Sensors. Adv Mater 28(5):795–831. https://doi.org/10.1002/adma.201503825
46. Yang S, Jiang C, S-h W (2017) Gas sensing in 2D materials. Appl Phys Rev 4(2):021304. https://doi.org/10.1063/1.4983310
47. Aswal DK, Gupta SK (2007) Science and Technology of Chemiresistor Gas Sensors. Nova Science Publishers, New York
48. Bishnoi A, Kumar S, Joshi N (2017) Chapter 9 - Wide-Angle X-ray Diffraction (WXRD): Technique for Characterization of Nanomaterials and Polymer Nanocomposites A2 - Thomas, Sabu. In: Zachariah AK, Mishra RK (eds) Thomas R. Microscopy Methods in Nanomaterials Characterization. Elsevier, Amsterdam, pp 313–337. https://doi.org/10.1016/B978-0-323-46141-2.00009-2
49. Ren Z, Guo Y, Liu C-H, Gao P-X (2013) Hierarchically nanostructured materials for sustainable environmental applications. Front Chem 1:18
50. Li J, Wang J, Wexler D, Shi D, Liang J, Liu H, Xiong S, Qian Y (2013) Simple synthesis of yolk-shelled ZnCo2O4 microspheres towards enhancing the electrochemical performance of lithium-ion batteries in conjunction with a sodium carboxymethyl cellulose binder. J Mater Chem A 1(48):15292–15299. https://doi.org/10.1039/c3ta13787b
51. Vuong NM, Chinh ND, Huy BT, Lee Y-I (2016) CuO-Decorated ZnO Hierarchical Nanostructures as Efficient and Established Sensing Materials for H2S Gas. Sensors 6:26736. https://doi.org/10.1038/srep26736 https://www.nature.com/articles/srep26736#supplementary-information
52. Bu-Yu Y, Ping-Fu H, Wenjea JT (2017) Enhanced room-temperature NO 2 gas sensing with TeO 2 /SnO 2 brush- and bead-like nanowire hybrid structures. Nanotechnology 28(4):045501
53. Joshi N, da Silva LF, Jadhav HS, Shimizu FM, Suman PH, M'Peko J-C, Orlandi MO, Seo JG, Mastelaro VR, Oliveira ON (2018) Yolk-shelled ZnCo2O4 microspheres: Surface properties and gas sensing application. Sensors Actuators B Chem 257(Supplement C):906–915. https://doi.org/10.1016/j.snb.2017.11.041
54. Li H, Yin Z, He Q, Li H, Huang X, Lu G, Fam DWH, Tok AIY, Zhang Q, Zhang H (2012) Fabrication of Single- and Multilayer MoS2 Film-Based Field-Effect Transistors for Sensing NO at Room Temperature. Small 8(1):63–67. https://doi.org/10.1002/smll.201101016
55. Gaiardo A, Fabbri B, Guidi V, Bellutti P, Giberti A, Gherardi S, Vanzetti L, Malagù C, Zonta G (2016) Metal Sulfides as Sensing Materials for Chemoresistive Gas Sensors. Sensors 16(3):296. https://doi.org/10.3390/s16030296
56. Cho S-Y, Koh H-J, Yoo H-W, Kim J-S, Jung H-T (2017) Tunable Volatile-Organic-Compound Sensor by Using Au Nanoparticle Incorporation on MoS2. ACS Sensors 2(1):183–189. https://doi.org/10.1021/acssensors.6b00801
57. Wee SH, Huang P-S, Lee J-K, Goyal A (2015) Heteroepitaxial Cu(2)O thin film solar cell on metallic substrates. Sci Report 5:16272. https://doi.org/10.1038/srep16272
58. Gao T, Huang P-S, Lee J-K, Leu PW (2015) Hierarchical metal nanomesh/microgrid structures for high performance transparent electrodes. RSC Adv 5(87):70713–70717. https://doi.org/10.1039/c5ra14851k
59. Joshi NJ, Grewal GS, Shrinet V, Pratap A, Buch NJ (2010) Synthesis and Characterization of Nano-Barium Titanate Prepared by Hydrothermal Process. Integr Ferroelectr 115(1):142–148. https://doi.org/10.1080/10584587.2010.496614
60. Xu N, Zhang Q, Yang H, Xia Y, Jiang Y (2017) In-situ preparation of hierarchical flower-like TiO2/carbon nanostructures as fillers for polymer composites with enhanced dielectric properties. 7:43970. https://doi.org/10.1038/srep43970
61. Singh A, Salmi Z, Jha P, Joshi N, Kumar A, Decorse P, Lecoq H, Lau-Truong S, Aswal DK, Gupta SK, Chehimi MM (2013) One step synthesis of highly ordered free standing flexible polypyrrole-silver nanocomposite films at air-water interface by photopolymerization. RSC Adv 3(32):13329–13336. https://doi.org/10.1039/c3ra40884a
62. Joshi NJ, Govindan TP, Shrinet V, Govindan TP, Pratap A (2012) Synthesis and dielectric behavior of nano-scale barium titanate. IEEE Trans Dielectr Electr Insul 19(1):83–90. https://doi.org/10.1109/TDEI.2012.6148505
63. Singh A, Salmi Z, Joshi N, Jha P, Decorse P, Lecoq H, Lau-Truong S, Jouini M, Aswal DK, Chehimi MM (2013) Electrochemical investigation of free-standing polypyrrole-silver nanocomposite films: a substrate free electrode material for supercapacitors. RSC Adv 3(46):24567–24575. https://doi.org/10.1039/C3RA42786B
64. Çelikbilek Ö, Jauffrès D, Siebert E, Dessemond L, Burriel M, Martin CL, Djurado E (2016) Rational design of hierarchically nanostructured electrodes for solid oxide fuel cells. J Power Sources 333:72–82. https://doi.org/10.1016/j.jpowsour.2016.09.156
65. Mahmoud BG, Khairy M, Rashwan FA, Foster CW, Banks CE (2016) Self-assembly of porous copper oxide hierarchical nanostructures for selective determinations of glucose and ascorbic acid. RSC Adv 6(18):14474–14482. https://doi.org/10.1039/c5ra22940e
66. Navale YH, Navale ST, Ramgir NS, Stadler FJ, Gupta SK, Aswal DK, Patil VB (2017) Zinc oxide hierarchical nanostructures as potential NO2 sensors. Sensors Actuators B Chem 251:551–563. https://doi.org/10.1016/j.snb.2017.05.085
67. Ou G, Fan P, Zhang H, Huang K, Yang C, Yu W, Wei H, Zhong M, Wu H, Li Y (2017) Large-scale hierarchical oxide nanostructures for high-performance electrocatalytic water splitting. Nano Energy 35:207–214. https://doi.org/10.1016/j.nanoen.2017.03.049
68. Huang P-S, Qin F, Xiong Z, Shim H-W, Gao T, Leu P, Lee J-K (2017) Novel Carrier Doping Mechanism for Transparent Conductor: Electron Donation from Embedded Ag Nanoparticles to the Oxide Matrix. ACS Appl Mater Interfaces 9(23):19973–19979. https://doi.org/10.1021/acsami.7b03871
69. Mishra YK, Adelung R (2017) ZnO tetrapod materials for functional applications. Mater Today. https://doi.org/10.1016/j.mattod.2017.11.003
70. Postica V, Gröttrup J, Adelung R, Lupan O, Mishra AK, de Leeuw NH, Ababii N, Carreira JFC, Rodrigues J, Sedrine NB, Correia MR, Monteiro T, Sontea V, Mishra YK (2017) Nanosensors: Multifunctional Materials: A Case Study of the Effects of Metal Doping on ZnO Tetrapods with Bismuth and Tin Oxides (Adv. Funct. Mater. 6/2017). Adv Funct Mater 27(6):n/a–n/a. https://doi.org/10.1002/adfm.201770036

71. Paulowicz I, Hrkac V, Kaps S, Cretu V, Lupan O, Braniste T, Duppel V, Tiginyanu I, Kienle L, Adelung R, Mishra YK (2015) Three-Dimensional SnO2 Nanowire Networks for Multifunctional Applications: From High-Temperature Stretchable Ceramics to Ultraresponsive Sensors. Adv Electron Mater 1(8):1500081–1500n/a. https://doi.org/10.1002/aelm.201500081
72. Kaps S, Bhowmick S, Gröttrup J, Hrkac V, Stauffer D, Guo H, Warren OL, Adam J, Kienle L, Minor AM, Adelung R, Mishra YK (2017) Piezoresistive Response of Quasi-One-Dimensional ZnO Nanowires Using an in Situ Electromechanical Device. ACS Omega 2(6):2985–2993. https://doi.org/10.1021/acsomega.7b00041
73. Tiginyanu I, Ghimpu L, Gröttrup J, Postolache V, Mecklenburg M, Stevens-Kalceff MA, Ursaki V, Payami N, Feidenhansl R, Schulte K, Adelung R, Mishra YK (2016) Strong light scattering and broadband (UV to IR) photoabsorption in stretchable 3D hybrid architectures based on Aerographite decorated by ZnO nanocrystallites. Sci Report 6:32913. https://doi.org/10.1038/srep32913 https://www.nature.com/articles/srep32913#supplementary-information
74. Jiang C, Zhang G, Wu Y, Li L, Shi K (2012) Facile synthesis of SnO2 nanocrystalline tubes by electrospinning and their fast response and high sensitivity to NOx at room temperature. Cryst Eng Comm 14(8):2739–2747. https://doi.org/10.1039/c2ce06405g
75. Wang Y, Jiang X, Xia Y (2003) A Solution-Phase, Precursor Route to Polycrystalline SnO2 Nanowires That Can Be Used for Gas Sensing under Ambient Conditions. J Am Chem Soc 125(52):16176–16177. https://doi.org/10.1021/ja037743f
76. Khun Khun K, Mahajan A, Bedi RK (2009) SnO2 thick films for room temperature gas sensing applications. J Appl Physiol 106(12):124509. https://doi.org/10.1063/1.3273323
77. Li Z, Wang N, Lin Z, Wang J, Liu W, Sun K, Fu YQ, Wang Z (2016) Room-Temperature High-Performance H2S Sensor Based on Porous CuO Nanosheets Prepared by Hydrothermal Method. ACS Appl Mater Interfaces 8(32):20962–20968. https://doi.org/10.1021/acsami.6b02893
78. Bhuvaneshwari S, Papachan S, Gopalakrishnan N (2017) Free standing CuO-MnO2 nanocomposite for room temperature ammonia sensing. AIP Conf Proc 1832(1):050126. https://doi.org/10.1063/1.4980359
79. Wang J, Wei L, Zhang L, Jiang C, Siu-Wai Kong E, Zhang Y (2012) Preparation of high aspect ratio nickel oxide nanowires and their gas sensing devices with fast response and high sensitivity. J Mater Chem 22(17):8327–8335. https://doi.org/10.1039/c2jm16934g
80. Jaisutti R, Lee M, Kim J, Choi S, Ha T-J, Kim J, Kim H, Park SK, Kim Y-H (2017) Ultrasensitive Room-Temperature Operable Gas Sensors Using p-Type Na:ZnO Nanoflowers for Diabetes Detection. ACS Appl Mater Interfaces 9(10):8796–8804. https://doi.org/10.1021/acsami.7b00673
81. Perfecto TM, Zito CA, Volanti DP (2017) Design of nanostructured WO3[middle dot]0.33H2O via combination of ultrasonic spray nozzle and microwave-assisted hydrothermal methods for enhancing isopropanol gas sensing at room temperature. Cryst Eng Comm 19(20):2733–2738. https://doi.org/10.1039/c7ce00523g
82. Gao J, Wu H, Zhou J, Yao L, Zhang G, Xu S, Xie Y, Li L, Shi K (2016) Mesoporous In2O3 nanocrystals: synthesis, characterization and NOx gas sensor at room temperature. New J Chem 40(2):1306–1311. https://doi.org/10.1039/c5nj02214b
83. Lupan O, Postica V, Wolff N, Polonskyi O, Duppel V, Kaidas V, Lazari E, Ababii N, Faupel F, Kienle L, Adelung R (2017) Localized Synthesis of Iron Oxide Nanowires and Fabrication of High Performance Nanosensors Based on a Single Fe2O3 Nanowire. Small 13(16):1602868–1602n/a. https://doi.org/10.1002/smll.201602868
84. Thirumalairajan S, Girija K, Mastelaro VR, Ponpandian N (2014) Surface Morphology-Dependent Room-Temperature LaFeO3 Nanostructure Thin Films as Selective NO2 Gas Sensor Prepared by Radio Frequency Magnetron Sputtering. ACS Appl Mater Interfaces 6(16):13917–13927. https://doi.org/10.1021/am503318y
85. Wu B, Wang L, Wu H, Kan K, Zhang G, Xie Y, Tian Y, Li L, Shi K (2016) Templated synthesis of 3D hierarchical porous Co3O4 materials and their NH3 sensor at room temperature. Microporous Mesoporous Mater 225:154–163. https://doi.org/10.1016/j.micromeso.2015.12.019
86. Xue X, Xing L, Chen Y, Shi S, Wang Y, Wang T (2008) Synthesis and H2S Sensing Properties of CuO−SnO2 Core/Shell PN-Junction Nanorods. J Phys Chem C 112(32):12157–12160. https://doi.org/10.1021/jp8037818
87. Bao M, Chen Y, Li F, Ma J, Lv T, Tang Y, Chen L, Xu Z, Wang T (2014) Plate-like p-n heterogeneous NiO/WO3 nanocomposites for high performance room temperature NO2 sensors. Nanoscale 6(8):4063–4066. https://doi.org/10.1039/C3NR05268K
88. Wang R, Yang S, Deng R, Chen W, Liu Y, Zhang H, Zakharova GS (2015) Enhanced gas sensing properties of V2O5 nanowires decorated with SnO2 nanoparticles to ethanol at room temperature. RSC Adv 5(51):41050–41058. https://doi.org/10.1039/C5RA00530B
89. Kim H-J, Lee J-H (2014) Highly sensitive and selective gas sensors using p-type oxide semiconductors: Overview. Sensors Actuators B Chem 192:607–627. https://doi.org/10.1016/j.snb.2013.11.005
90. Lee J-H (2009) Gas sensors using hierarchical and hollow oxide nanostructures: Overview. Sensors Actuators B Chem 140(1):319–336. https://doi.org/10.1016/j.snb.2009.04.026
91. Sinha M, Mahapatra R, Mondal B, Maruyama T, Ghosh R (2016) Ultrafast and Reversible Gas-Sensing Properties of ZnO Nanowire Arrays Grown by Hydrothermal Technique. J Phys Chem C 120(5):3019–3025. https://doi.org/10.1021/acs.jpcc.5b11012
92. Tesfamichael T, Cetin C, Piloto C, Arita M, Bell J (2015) The effect of pressure and W-doping on the properties of ZnO thin films for NO2 gas sensing. Appl Surf Sci 357:728–734. https://doi.org/10.1016/j.apsusc.2015.08.248
93. Schedin F, Geim AK, Morozov SV, Hill EW, Blake P, Katsnelson MI, Novoselov KS (2007) Detection of individual gas molecules adsorbed on graphene. Nat Mater 6(9):652–655 http://www.nature.com/nmat/journal/v6/n9/suppinfo/nmat1967_S1.html
94. Yuan W, Shi G (2013) Graphene-based gas sensors. J Mater Chem A 1(35):10078–10091. https://doi.org/10.1039/c3ta11774j
95. Yoon HJ, Jun DH, Yang JH, Zhou Z, Yang SS, Cheng MM-C (2011) Carbon dioxide gas sensor using a graphene sheet. Sensors Actuators B Chem 157(1):310–313. https://doi.org/10.1016/j.snb.2011.03.035
96. Ren Y, Zhu C, Cai W, Li H, Ji H, Kholmanov I, Wu Y, Piner RD, Ruoff RS (2012) Detection of sulfur dioxide gas with graphene field effect transistor. Appl Phys Lett 100(16):163114. https://doi.org/10.1063/1.4704803
97. Kumar B, Min K, Bashirzadeh M, Farimani AB, Bae MH, Estrada D, Kim YD, Yasaei P, Park YD, Pop E, Aluru NR, Salehi-Khojin A (2013) The Role of External Defects in Chemical Sensing of Graphene Field-Effect Transistors. Nano Lett 13(5):1962–1968. https://doi.org/10.1021/nl304734g
98. Kang I-S, So H-M, Bang G-S, Kwak J-H, Lee J-O, Won Ahn C (2012) Recovery improvement of graphene-based gas sensors functionalized with nanoscale heterojunctions. Appl Phys Lett 101(12):123504. https://doi.org/10.1063/1.4753974
99. Muhammad Hafiz S, Ritikos R, Whitcher TJ, Md Razib N, DCS B, Chanlek N, Nakajima H, Saisopa T, Songsiriritthigul P, Huang

NM, Rahman SA (2014) A practical carbon dioxide gas sensor using room-temperature hydrogen plasma reduced graphene oxide. Sensors Actuators B Chem 193(Supplement C):692–700. https://doi.org/10.1016/j.snb.2013.12.017
100. Geim AK, Novoselov KS (2007) The rise of graphene. Nat Mater 6(3):183–191
101. Novoselov KS, Falko VI, Colombo L, Gellert PR, Schwab MG, Kim K (2012) A roadmap for graphene. Nature 490(7419):192–200
102. Rigoni F, Maiti R, Baratto C, Donarelli M, MacLeod J, Gupta B, Lyu M, Ponzoni A, Sberveglieri G, Motta N, Faglia G (2017) Transfer of CVD-grown graphene for room temperature gas sensors. Nanotechnology 28(41):414001
103. Sysoev VI, Bulusheva LG, Asanov IP, Shubin YV, Okotrub AV (2016) Thermally exfoliated fluorinated graphite for NO2 gas sensing. Phys Status Solidi B 253(12):2492–2498. https://doi.org/10.1002/pssb.201600270
104. Bo Z, Shuai X, Mao S, Yang H, Qian J, Chen J, Yan J, Cen K (2014) Green preparation of reduced graphene oxide for sensing and energy storage applications. 4:4684. https://doi.org/10.1038/srep04684. https://www.nature.com/articles/srep04684#supplementary-information
105. Tan C, Zhang H (2015) Epitaxial Growth of Hetero-Nanostructures Based on Ultrathin Two-Dimensional Nanosheets. J Am Chem Soc 137(38):12162–12174. https://doi.org/10.1021/jacs.5b03590
106. Wang T, Huang D, Yang Z, Xu S, He G, Li X, Hu N, Yin G, He D, Zhang L (2016) A Review on Graphene-Based Gas/Vapor Sensors with Unique Properties and Potential Applications. Nano-Micro Lett 8(2):95–119. https://doi.org/10.1007/s40820-015-0073-1
107. Strudwick AJ, Weber NE, Schwab MG, Kettner M, Weitz RT, Wünsch JR, Müllen K, Sachdev H (2015) Chemical Vapor Deposition of High Quality Graphene Films from Carbon Dioxide Atmospheres. ACS Nano 9(1):31–42. https://doi.org/10.1021/nn504822m
108. Yan K, Fu L, Peng H, Liu Z (2013) Designed CVD Growth of Graphene via Process Engineering. Acc Chem Res 46(10):2263–2274. https://doi.org/10.1021/ar400057n
109. Yavari F, Koratkar N (2012) Graphene-Based Chemical Sensors. J Phys Chem Lett 3(13):1746–1753. https://doi.org/10.1021/jz300358t
110. Lee S-K, Jang HY, Jang S, Choi E, Hong BH, Lee J, Park S, Ahn J-H (2012) All Graphene-Based Thin Film Transistors on Flexible Plastic Substrates. Nano Lett 12(7):3472–3476. https://doi.org/10.1021/nl300948c
111. Yan C, Cho JH, Ahn J-H (2012) Graphene-based flexible and stretchable thin film transistors. Nanoscale 4(16):4870–4882. https://doi.org/10.1039/c2nr30994g
112. Park SJ, Kwon OS, Lee SH, Song HS, Park TH, Jang J (2012) Ultrasensitive Flexible Graphene Based Field-Effect Transistor (FET)-Type Bioelectronic Nose. Nano Lett 12(10):5082–5090. https://doi.org/10.1021/nl301714x
113. Liu Y, Chang J, Lin L (2014) A flexible graphene FET gas sensor using polymer as gate dielectrics. Paper presented at the IEEE 27th International Conference on Micro Electro Mechanical Systems (MEMS), San Francisco, CA, USA
114. Liu Y, Lin, S. and Lin, L. (2015) A versatile gas sensor with selectivity using a single graphene transistor. Paper presented at the 2015 18th International Conference on Solid-State Sensors, Actuators and Microsystems (TRANSDUCERS)
115. Xia F, Mueller T, Golizadeh-Mojarad R, Freitag M, Lin Y-M, Tsang J, Perebeinos V, Avouris P (2009) Photocurrent Imaging and Efficient Photon Detection in a Graphene Transistor. Nano Lett 9(3):1039–1044. https://doi.org/10.1021/nl8033812
116. Liu Y, Yu J, Cui Y, Hayasaka T, Liu H, Li X, Lin L (2017) An AC sensing scheme for minimal baseline drift and fast recovery on graphene FET gas sensor. Paper presented at the 2017 19th International Conference on Solid-State Sensors, Actuators and Microsystems (TRANSDUCERS)
117. Liu C, Kuang Q, Xie Z, Zheng L (2015) The effect of noble metal (Au, Pd and Pt) nanoparticles on the gas sensing performance of SnO2-based sensors: a case study on the {221} high-index faceted SnO2 octahedra. Cryst Eng Comm 17(33):6308–6313. https://doi.org/10.1039/c5ce01162k
118. Korotcenkov G (2013) Handbook of Gas Sensor Materials: Properties, Advantages and Shortcomings for Applications Volume 2: New Trends and Technologies. Springer, New York
119. Tricoli A (2012) Structural Stability and Performance of Noble Metal-Free SnO(2)-Based Gas Sensors. Bio Sensors 2(2):221–233. https://doi.org/10.3390/bios2020221
120. Latif U, Dickert FL (2015) Graphene Hybrid Materials in Gas Sensing Applications. Sensors (Basel, Switzerland) 15(12):30504–30524. https://doi.org/10.3390/s151229814
121. Ganhua L, Leonidas EO, Junhong C (2009) Reduced graphene oxide for room-temperature gas sensors. Nanotechnology 20(44):445502
122. Gupta Chatterjee S, Chatterjee S, Ray AK, Chakraborty AK (2015) Graphene–metal oxide nanohybrids for toxic gas sensor: A review. Sensors Actuators B Chem 221(Supplement C):1170–1181. https://doi.org/10.1016/j.snb.2015.07.070
123. Gu F, Nie R, Han D, Wang Z (2015) In2O3–graphene nanocomposite based gas sensor for selective detection of NO2 at room temperature. Sensors Actuators B Chem 219(Supplement C):94–99. https://doi.org/10.1016/j.snb.2015.04.119
124. Enoch N, Rajesh N, Yuhua X, Yunxiang G, Mei Z, Liming D (2013) Sensor arrays from multicomponent micropatterned nanoparticles and graphene. Nanotechnology 24(44):444010
125. Song Z, Wei Z, Wang B, Luo Z, Xu S, Zhang W, Yu H, Li M, Huang Z, Zang J, Yi F, Liu H (2016) Sensitive Room-Temperature H2S Gas Sensors Employing SnO2 Quantum Wire/Reduced Graphene Oxide Nanocomposites. Chem Mater 28(4):1205–1212. https://doi.org/10.1021/acs.chemmater.5b04850
126. Ghosh R, Midya A, Santra S, Ray SK, Guha PK (2013) Chemically Reduced Graphene Oxide for Ammonia Detection at Room Temperature. ACS Appl Mater Interfaces 5(15):7599–7603. https://doi.org/10.1021/am4019109
127. Kumar R, Avasthi DK, Kaur A (2017) Fabrication of chemiresistive gas sensors based on multistep reduced graphene oxide for low parts per million monitoring of sulfur dioxide at room temperature. Sensors Actuators B Chem 242:461–468. https://doi.org/10.1016/j.snb.2016.11.018
128. Huang L, Wang Z, Zhang J, Pu J, Lin Y, Xu S, Shen L, Chen Q, Shi W (2014) Fully Printed, Rapid-Response Sensors Based on Chemically Modified Graphene for Detecting NO2 at Room Temperature. ACS Appl Mater Interfaces 6(10):7426–7433. https://doi.org/10.1021/am500843p
129. Zhang D, Liu A, Chang H, Xia B (2015) Room-temperature high-performance acetone gas sensor based on hydrothermal synthesized SnO2-reduced graphene oxide hybrid composite. RSC Adv 5(4):3016–3022. https://doi.org/10.1039/c4ra10942b
130. Acharyya D, Bhattacharyya P (2016) Highly Efficient Room-Temperature Gas Sensor Based on TiO₂ Nanotube-Reduced Graphene-Oxide Hybrid Device. IEEE Electron Device Letters 37(5):656–659. https://doi.org/10.1109/led.2016.2544954
131. Zhang D, Liu J, Jiang C, Liu A, Xia B (2017) Quantitative detection of formaldehyde and ammonia gas via metal oxide-modified graphene-based sensor array combining with neural network model. Sensors Actuators B Chem 240:55–65. https://doi.org/10.1016/j.snb.2016.08.085
132. Xia Y, Wang J, Xu J-L, Li X, Xie D, Xiang L, Komarneni S (2016) Confined Formation of Ultrathin ZnO Nanorods/Reduced Graphene Oxide Mesoporous Nanocomposites for High-

Performance Room-Temperature NO2 Sensors. ACS Appl Mater Interfaces 8(51):35454–35463. https://doi.org/10.1021/acsami.6b12501
133. Zhang D, Jiang C, Liu J, Cao Y (2017) Carbon monoxide gas sensing at room temperature using copper oxide-decorated graphene hybrid nanocomposite prepared by layer-by-layer self-assembly. Sensors Actuators B Chem 247:875–882. https://doi.org/10.1016/j.snb.2017.03.108
134. Su P-G, Peng S-L (2015) Fabrication and NO2 gas-sensing properties of reduced graphene oxide/WO3 nanocomposite films. Talanta 132:398–405. https://doi.org/10.1016/j.talanta.2014.09.034
135. Chen N, Li X, Wang X, Yu J, Wang J, Tang Z, Akbar SA (2013) Enhanced room temperature sensing of Co3O4-intercalated reduced graphene oxide based gas sensors. Sensors Actuators B Chem 188:902–908. https://doi.org/10.1016/j.snb.2013.08.004
136. Zhang J, Zeng D, Zhao S, Wu J, Xu K, Zhu Q, Zhang G, Xie C (2015) Room temperature NO2 sensing: what advantage does the rGO-NiO nanocomposite have over pristine NiO? Phys Chem Chem Phys 17(22):14903–14911. https://doi.org/10.1039/C5CP01987G
137. Gu F, Nie R, Han D, Wang Z (2015) In2O3–graphene nanocomposite based gas sensor for selective detection of NO2 at room temperature. Sensors Actuators B Chem 219:94–99. https://doi.org/10.1016/j.snb.2015.04.119
138. Tan TL, Ng M-F, Eda G (2016) Stable Monolayer Transition Metal Dichalcogenide Ordered Alloys with Tunable Electronic Properties. J Phys Chem C 120(5):2501–2508. https://doi.org/10.1021/acs.jpcc.5b10739
139. Jeong H, Oh HM, Gokarna A, Kim H, Yun SJ, Han GH, Jeong MS, Lee YH, Lerondel G (2017) Integrated Freestanding Two-dimensional Transition Metal Dichalcogenides. Adv Mater 29(18):1700308–1700n/a. https://doi.org/10.1002/adma.201700308
140. Chhowalla M, Liu Z, Zhang H (2015) Two-dimensional transition metal dichalcogenide (TMD) nanosheets. Chem Soc Rev 44(9):2584–2586. https://doi.org/10.1039/c5cs90037a
141. Manzeli S, Ovchinnikov D, Pasquier D, Yazyev OV, Kis A (2017) 2D transition metal dichalcogenides. 2:17033. https://doi.org/10.1038/natrevmats.2017.33
142. Bhimanapati GR, Lin Z, Meunier V, Jung Y, Cha J, Das S, Xiao D, Son Y, Strano MS, Cooper VR, Liang L, Louie SG, Ringe E, Zhou W, Kim SS, Naik RR, Sumpter BG, Terrones H, Xia F, Wang Y, Zhu J, Akinwande D, Alem N, Schuller JA, Schaak RE, Terrones M, Robinson JA (2015) Recent Advances in Two-Dimensional Materials beyond Graphene. ACS Nano 9(12):11509–11539. https://doi.org/10.1021/acsnano.5b05556
143. Mak KF, Shan J (2016) Photonics and optoelectronics of 2D semiconductor transition metal dichalcogenides. Nat Photon 10(4):216–226. https://doi.org/10.1038/nphoton.2015.282
144. Susarla S, Kutana A, Hachtel JA, Kochat V, Apte A, Vajtai R, Idrobo JC, Yakobson BI, Tiwary CS, Ajayan PM (2017) Quaternary 2D Transition Metal Dichalcogenides (TMDs) with Tunable Bandgap. Adv Mater 29(35):1702457–1702n/a. https://doi.org/10.1002/adma.201702457
145. Velusamy DB, Kim RH, Cha S, Huh J, Khazaeinezhad R, Kassani SH, Song G, Cho SM, Cho SH, Hwang I, Lee J, Oh K, Choi H, Park C (2015) Flexible transition metal dichalcogenide nanosheets for band-selective photodetection. 6:8063. https://doi.org/10.1038/ncomms9063. https://www.nature.com/articles/ncomms9063#supplementary-information
146. Perkins FK, Friedman AL, Cobas E, Campbell PM, Jernigan GG, Jonker BT (2013) Chemical Vapor Sensing with Monolayer MoS2. Nano Lett 13(2):668–673. https://doi.org/10.1021/nl3043079
147. Liu B, Chen L, Liu G, Abbas AN, Fathi M, Zhou C (2014) High-Performance Chemical Sensing Using Schottky-Contacted Chemical Vapor Deposition Grown Monolayer MoS2 Transistors. ACS Nano 8(5):5304–5314. https://doi.org/10.1021/nn5015215
148. Nam H, Oh B-R, Chen P, Chen M, Wi S, Wan W, Kurabayashi K, Liang X (2015) Multiple MoS2 Transistors for Sensing Molecule Interaction Kinetics. 5:10546. https://doi.org/10.1038/srep10546. https://www.nature.com/articles/srep10546#supplementary-information
149. Cho B, Hahm MG, Choi M, Yoon J, Kim AR, Lee Y-J, Park S-G, Kwon J-D, Kim CS, Song M, Jeong Y, Nam K-S, Lee S, Yoo TJ, Kang CG, Lee BH, Ko HC, Ajayan PM, Kim D-H (2015) Charge-transfer-based Gas Sensing Using Atomic-layer MoS2. 5:8052. https://doi.org/10.1038/srep08052. https://www.nature.com/articles/srep08052#supplementary-information
150. Bergeron H, Sangwan VK, McMorrow JJ, Campbell GP, Balla I, Liu X, Bedzyk MJ, Marks TJ, Hersam MC (2017) Chemical vapor deposition of monolayer MoS2 directly on ultrathin Al2O3 for low-power electronics. Appl Phys Lett 110(5):053101. https://doi.org/10.1063/1.4975064
151. Tao H, Zhang Y, Gao Y, Sun Z, Yan C, Texter J (2017) Scalable exfoliation and dispersion of two-dimensional materials - an update. Phys Chem Chem Phys 19(2):921–960. https://doi.org/10.1039/c6cp06813h
152. Kim HT, Kim HY, Park YS, Kim YS, Jang WH (2017) Two-Dimensional Transition Metal Disulfides for Chemoresistive Gas Sensing: Perspective and Challenges. Chemosensors 5(2). https://doi.org/10.3390/chemosensors5020015
153. Cho B, Kim AR, Park Y, Yoon J, Lee Y-J, Lee S, Yoo TJ, Kang CG, Lee BH, Ko HC, Kim D-H, Hahm MG (2015) Bifunctional Sensing Characteristics of Chemical Vapor Deposition Synthesized Atomic-Layered MoS2. ACS Appl Mater Interfaces 7(4):2952–2959. https://doi.org/10.1021/am508535x
154. Lee K, Gatensby R, McEvoy N, Hallam T, Duesberg GS (2013) High-Performance Sensors Based on Molybdenum Disulfide Thin Films. Adv Mater 25(46):6699–6702. https://doi.org/10.1002/adma.201303230
155. Cho B, Hahm MG, Choi M, Yoon J, Kim AR, Lee Y-J, Park S-G, Kwon J-D, Kim CS, Song M, Jeong Y, Nam K-S, Lee S, Yoo TJ, Kang CG, Lee BH, Ko HC, Ajayan PM, Kim D-H (2015) Charge-transfer-based Gas Sensing Using Atomic-layer MoS(2). Sci Reports 5:8052. https://doi.org/10.1038/srep08052
156. Baek J, Yin D, Liu N, Omkaram I, Jung C, Im H, Hong S, Kim SM, Hong YK, Hur J, Yoon Y, Kim S (2017) A highly sensitive chemical gas detecting transistor based on highly crystalline CVD-grown MoSe2 films. Nano Res 10(6):1861–1871. https://doi.org/10.1007/s12274-016-1291-7
157. Ko KY, Song J-G, Kim Y, Choi T, Shin S, Lee CW, Lee K, Koo J, Lee H, Kim J, Lee T, Park J, Kim H (2016) Improvement of Gas-Sensing Performance of Large-Area Tungsten Disulfide Nanosheets by Surface Functionalization. ACS Nano 10(10):9287–9296. https://doi.org/10.1021/acsnano.6b03631
158. Cihan K, Duyoung C, Alireza K, Chin Hung L, Serdar Y, Chulmin C, Sungho J, Prabhakar RB (2016) High-performance flexible hydrogen sensor made of WS 2 nanosheet–Pd nanoparticle composite film. Nanotechnol 27(19):195501
159. Ou JZ, Ge W, Carey B, Daeneke T, Rotbart A, Shan W, Wang Y, Fu Z, Chrimes AF, Wlodarski W, Russo SP, Li YX, Kalantar-zadeh K (2015) Physisorption-Based Charge Transfer in Two-Dimensional SnS2 for Selective and Reversible NO2 Gas Sensing. ACS Nano 9(10):10313–10323. https://doi.org/10.1021/acsnano.5b04343
160. Zhang D, Wu J, Li P, Cao Y (2017) Room-temperature SO2 gas-sensing properties based on a metal-doped MoS2 nanoflower: an

experimental and density functional theory investigation. J Mater Chem A 5(39):20666–20677. https://doi.org/10.1039/c7ta07001b
161. Qin Z, Ouyang C, Zhang J, Wan L, Wang S, Xie C, Zeng D (2017) 2D WS2 nanosheets with TiO2 quantum dots decoration for high-performance ammonia gas sensing at room temperature. Sensors Actuators B Chem 253(Supplement C):1034–1042. https://doi.org/10.1016/j.snb.2017.07.052
162. Zhang D, Jiang C, Sun Ye (2017) Room-temperature high-performance ammonia gas sensor based on layer-by-layer self-assembled molybdenum disulfide/zinc oxide nanocomposite film. J Alloys Compd 698:476-483. https://doi.org/10.1016/j.jallcom.2016.12.222
163. Cui S, Wen Z, Huang X, Chang J, Chen J (2015) Stabilizing MoS2 Nanosheets through SnO2 Nanocrystal Decoration for High-Performance Gas Sensing in Air. Small 11(19):2305–2313. https://doi.org/10.1002/smll.201402923
164. Li X, Wang J, Xie D, Xu J, Xia Y, Xiang L, Komarneni S (2017) Reduced graphene oxide/MoS2 hybrid films for room-temperature formaldehyde detection. Mater Lett 189:42–45. https://doi.org/10.1016/j.matlet.2016.11.046
165. Li X, Li X, Li Z, Wang J, Zhang J (2017) WS2 nanoflakes based selective ammonia sensors at room temperature. Sensors Actuators B Chem 240:273–277. https://doi.org/10.1016/j.snb.2016.08.163
166. Weidong S, Lihua H, Haishui W, Hongjie Z, Jianhui Y, Pinghui W (2006) Hydrothermal growth and gas sensing property of flower-shaped SnS2 nanostructures. Nanotechnol 17(12):2918
167. Late DJ, Doneux T, Bougouma M (2014) Single-layer MoSe2 based NH3 gas sensor. Appl Phys Lett 105(23):233103. https://doi.org/10.1063/1.4903358
168. Liu H, Liu Y, Chu Y, Hayasaka T, Joshi N, Cui Y, Wang X, You Z, Lin LAC phase sensing of graphene FETs for chemical vapors with fast recovery and minimal baseline drift. Sensors Actuators B Chem. https://doi.org/10.1016/j.snb.2018.01.244
169. Chang Y, Tang N, Qu H, Liu J, Zhang D, Zhang H, Pang W, Duan X (2016) Detection of Volatile Organic Compounds by Self-assembled Monolayer Coated Sensor Array with Concentration-independent Fingerprints. Sci Report 6:23970. https://doi.org/10.1038/srep23970 https://www.nature.com/articles/srep23970#supplementary-information
170. Kahn N, Lavie O, Paz M, Segev Y, Haick H (2015) Dynamic Nanoparticle-Based Flexible Sensors: Diagnosis of Ovarian Carcinoma from Exhaled Breath. Nano Lett 15(10):7023–7028. https://doi.org/10.1021/acs.nanolett.5b03052
171. Liu Y (2017) Room Temperature Gas Sensing using Graphene FET. Dissertation. University of California, Berkeley